Atmospheric Pollution Research 15 (2024) 102088

Contents lists available at ScienceDirect

Atmospheric Pollution Research

journal homepage: www.elsevier.com/locate/apr

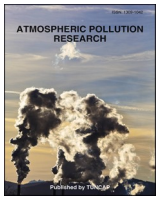

Black carbon instrument responses to laboratory generated particles

Laura Salo [a,*], Karri Saarnio [b], Sanna Saarikoski [b], Kimmo Teinilä [b], Luis M.F. Barreira [b], Petteri Marjanen [a], Sampsa Martikainen [a], Helmi Keskinen [a], Katja Mustonen [a], Teemu Lepistö [a], Päivi Aakko-Saksa [c], Henri Hakkarainen [d], Tobias Pfeiffer [e], Pasi Jalava [d], Panu Karjalainen [a], Jorma Keskinen [a], Niina Kuittinen [a], Hilkka Timonen [b], Topi Rönkkö [a]

[a] Aerosol Physics Laboratory, Physics Unit, Tampere University, P.O. Box 692, 33014 Tampere, Finland
[b] Atmospheric Composition Research, Finnish Meteorological Institute, P.O. Box 503, 00101 Helsinki, Finland
[c] VTT Technical Research Centre of Finland, P.O. Box 1000, 02044 Espoo, Finland
[d] Inhalation toxicology laboratory, Department of Environmental and Biological Sciences, University of Eastern Finland, P.O. Box 1627, 70211 Kuopio, Finland
[e] VSParticle B.V., Oostsingel 209, 2612HL Delft, the Netherlands

ARTICLE INFO

Keywords:
Soot
MSS
AE33
MAAP
SP-AMS

ABSTRACT

Accurate measurement of black carbon (BC) particles is vital for climate models as well as air quality assessments. While the need for BC particle measurement has been recognized, standardization of instruments and procedures for ambient measurement is still underway. In this study, we used laboratory generated soot particles to assess nine instruments targeting BC mass concentration measurement. The measurement matrix included different BC concentrations (ranging from atmospheric levels to combustion emission levels), different particle coatings, two particle sources (gas burner and spark generator) and two dilution methods. The nine instruments included six different models: aethalometers AE33 and MA200, thermo-optical OC-EC analysis, multi-angle absorption photometer MAAP 5012, photoacoustic instrument MSS, and soot particle aerosol mass spectrometer SP-AMS. The main discrepancy we observed was that the SP-AMS results were systematically lower, approximately only half of the BC measured by other instruments. A portion of this is explained by particle losses in the aerodynamic lens of the SP-AMS and the parameters used in the data analysis. Some smaller discrepancies were identified for the other instruments, but overall, the median values from were within 25 % of each other. Instruments' operation principles and covered concentration ranges need to be carefully considered especially in emission measurements where the aerosols can have high temporal variation as well as high BC concentrations. In general, the results can decrease the uncertainties in climate and air quality studies by providing tools for more accurate and comparable BC measurements and when the existing BC data is interpreted.

1. Introduction

Black carbon (BC) is a common atmospheric pollutant, resulting from incomplete combustion (see e.g., Lighty et al., 2000; Michelsen et al., 2020). The most common source of BC in a modern urban environment is traffic, i.e., vehicles equipped with internal combustion engines; other common sources are coal and biomass combustion (Briggs and Long, 2016; Liu et al., 2018; Rönkkö et al., 2023; Saarikoski et al., 2021). A historical example of how BC can affect air quality is the "Big Smoke" in 1952 in London, where the combination of meteorological conditions and heavy coal-burning resulted in so much smoke in the city, that visibility was reduced to a few meters and at least 6000 people died as a direct consequence (Stone, 2002). Recent analysis of filters collected in London in the 1950's have revealed weekday average BC concentrations of up to 250 μg/m^3 (ten Brink et al., 2022).

Despite improvements in combustion technology and an overall trend towards cleaner energy sources, BC remains a major component of ambient aerosols around the world (Klimont et al., 2017); the population weighted exposure to BC is estimated at 2.14 μg/m^3 (Wang et al., 2014), but in highly polluted areas, such as New Delhi, India, exposure can be ten times this amount (Pant et al., 2017). The World Health Organization (WHO) has acknowledged BC as a health risk and

Peer review under responsibility of Turkish National Committee for Air Pollution Research and Control.
* Corresponding author.
E-mail address: laura.salo@tuni.fi (L. Salo).

https://doi.org/10.1016/j.apr.2024.102088
Received 29 September 2023; Received in revised form 31 January 2024; Accepted 16 February 2024
Available online 17 February 2024

recommends systematic BC measurements, although specific target levels have not yet been established due to limited data (World Health Organization, 2021). In addition to health, BC also impacts our climate: it efficiently absorbs light thus contributing positively to radiative forcing in the atmosphere. However, BC particles are also condensation nuclei for cloud-forming water droplets, which can in turn contribute to radiative forcing in either direction. The net effect of BC particles on the global climate remains unclear; however, studies suggest that the faster warming of the arctic compared to overall global warming is at least in part due to BC particles (Bond et al., 2013; Räisänen et al., 2022).

Currently there are no standardized methods for traceable calibration of BC measurement methods. BC also does not have an unambiguous chemical definition, which complicates describing a standard. A definition of BC given by Petzold et al. (2013) includes five attributes: graphite-like microstructure, agglomerate of smaller carbon spheres, thermally stable, insoluble and strongly light-absorbing. They give further definitions relating to the way that BC is measured. Thermally measured corresponds to elemental carbon (EC), when BC is optically measured the correct term is equivalent BC (eBC) and when laser-induced incandescence is used it is called refractory BC (rBC), also a form of equivalent BC. Additionally, the terms soot and BC are sometimes used interchangeably, soot being a more common term in literature regarding emission measurement and referring to the solid component of exhaust aerosol, consisting mostly of BC. None of the above methods encompass the full definition of BC; as a result, they are not expected to result in the exact same response to BC particles, nor does any single method give the "true" BC concentration. Results can depend upon the particle concentration, size, morphology, and the presence of other compounds either coating the BC particles or as separate particles.

EC is measured thermo-optically by collecting particles onto a quartz filter, then heating the sample, and measuring the released vapors, with vapors released at the highest temperature assumed to be from EC. The heating is in two steps: first in an oxygen-free environment to remove most of organic carbon and decompose inorganic carbonates from the sample; and second in an oxygen-containing environment to oxidize into CO2 the EC and the organics pyrolytically converted to EC in the first step, which is ultimately converted to methane and measured by FID. Currently, thermo-optical measurement is the suggested reference for measuring BC in ambient aerosol in the EU (Cavalli et al., 2010). The main drawback is that this is an off-line method, and the collection time and sample collection volume must be large enough to capture a measurable amount of EC.

Optical instruments rely on the highly absorbing nature of BC. Two examples of optical devices are the aethalometers and MAAPs (Multi-Angle Absorption Photometer). Aethalometers use filters to collect particles and measure the dimming of light through the filter, reporting the eBC concentration in real time (Hansen et al., 1984). MAAPs are similar to aethalometers, collecting particles onto a filter, however, reflected light is measured in addition to transmitted light (Petzold et al., 2002). In theory, MAAPs should be more accurate, as they can distinguish between scattering and absorption. Grouped with optical methods is also photoacoustic spectrometry (PAS). PAS uses an intensity modulated light-source directed at the particles. The periodical heating and cooling of the particles produces an acoustic wave, which is then detected (Petzold and Niessner, 1996).

Three examples of the rBC measurement type is the Laser-Induced Incandescence (LII) instrument (Snelling et al., 2005; Vander Wal and Weiland, 1994), the single-particle soot photometer (SP2), and SP-AMS (Soot Particle Aerosol Mass Spectrometer). LII measures both the light absorbed by particles and when the particles heat up, the emitted radiation. The SP2 also employs laser-induced incandescence and measures the resulting radiation to determine the rBC mass concentration; however, it measures single particles and is thus able to also measure number concentration (Sedlacek, 2017). The SP2 also detects scattering at 1064 nm, which can be used to detect particle coatings (Sedlacek, 2017). The BC signal from a mass spectrometer is also referred to as rBC, as a laser is used to vaporize the particles (Onasch et al., 2012). In aerosol mass spectrometers, the detection of the particles is done separately (in the same way as particles of other chemical compositions), by ionizing the vaporized sample and moving it through an electrical field onto a detection plate, where an electrical signal is recorded. The particle chemistry is inferred from the mass to charge ratio.

Many comparison studies have been conducted to investigate differences between instruments (Aakko-Saksa et al., 2022; Cuesta--Mosquera et al., 2021; Kalbermatter et al., 2022; Kinsey et al., 2019; Müller et al., 2011; Slowik et al., 2007). Slowik et al. (2007) showed that uncoated soot particles caused a larger signal in MAAP than PAS, and while particle orientation was speculated as a possible cause, no conclusion was reached. Another known obstacle is the lensing effect (Kanaya et al., 2008). BC particles coated by organic material may appear larger to optical instruments, as the coating acts as a lens focusing light onto the particle and resulting in a higher reading for BC mass. Kalbermatter et al. (2022) found significant differences in instrument responses depending on the amount of coating, with filter-based measurement overestimating the BC content. Slowik et al. (2007) found that oleic acid coating did not affect the comparison between PAS and MAAP, whereas a thick anthracene coating increased the MAAP signal compared to PAS (but a thin coating did not). The Müller et al. (2011) study included altogether twenty different instruments (MAAPs, aethalometers and Particle Soot Absorption Photometers (PSAPs)), all using optical methods. They found that MAAPs were the most consistent when compared to each other, with only 3 % variability. The variability in the PSAPs (8 %–27 %) and aethalometers (20 %) was found to be at least in part due to variation in the spot size. Drinovec et al. (2022) showed that aethalometers are especially susceptible to scattering artifacts for particles below 70 nm and Yus-Díez et al. showed that the multiple-scattering correction factor depends on the filter tape material. The study by Kinsey et al. (2019) found that LII overestimated and MSS underestimated the concentration of BC emissions of a turboshaft engine. Furthermore, both instruments were shown to be sensitive to particle size, especially particles smaller than 30 nm. Aakko-Saksa et al. (2022) studied instrument performance (LII, PAS, smoke meter, MAAP, aethalometer and EC thermo-optical analysis) with marine engine emitted aerosol. Overall, they found good agreement between the instruments; however, the presence of sulfur in the fuel increased differences. Cuesta-Mosquera et al. noted in their comparison of 23 aethalometer units that the tape should be allowed to advance a few times before regarding data as valid, as the instrument updates compensation parameters based on measurements from the previous spot.

In our study, we used a gas burner to generate combustion-originated aerosol and sample it with six different BC instruments, three of which were in pairs, to detect any variation between identical instruments. The aerosol sample was taken either as is, or a sample treatment was applied to simulate either primary aerosol (hot exhaust) or aerosol which has aged in the atmosphere. Other additional parameters were the addition of hydrocarbons or sulfuric acid into the sample to produce coated BC particles. We also studied whether the laboratory soot generation was affected by the dilution method, by using two diluter systems. Finally, we examined whether a spark generator could be used as a substitute for combustion-generated soot in a laboratory setting. To clarify, the objectives of this study were.

1. Compare BC instrument responses to laboratory-generated soot with different sample treatments and particle coatings
2. Compare the instrument response dependency on the dilution method
3. Compare the properties of gas burner and spark generator generated particles as measured by the BC instruments

2. Materials & methods

This study involved approximately four weeks of laboratory measurements. In this section we describe the measurement setup and measurement matrix, as well as the studied instruments. We also go through any instrument-specific data processing and corrections made to the data.

2.1. Measurement setup and matrix

A simplified version of the aerosol production setup is shown in Fig. 1, the full setup is included in Fig. S1. We produced particles with either a flat flame burner (McKenna Products) fueled with acetylene (normal case), or a spark generator (VSP-G1, VSParticle B.V.) equipped with two carbon electrodes. The gas burner emissions were drawn from the flue pipe using an ejector diluter, simultaneously diluting the flue gas with air. At this point SO_2 could be added, which would then convert into sulfuric acid in the oxidation catalyst. After the catalyst, either benzene droplets or octacosane vapor could be added to the aerosol mixture. Next, the aerosol was diluted using either a porous tube diluter (PTD) combined with residence time tube (RTT), normal case, or two consecutive ejector diluters (eDiluter Pro, Dekati Ltd.), the first a hot diluter and the second operating at ambient temperature. Next was the sample treatment. It determines whether the aerosol is considered primary, fresh, or aged. These terms refer to an emission aerosol before it is released into ambient air (primary), a few seconds after diluting in ambient conditions (fresh) and after hours to days in the atmosphere (aged) (see, e.g., Rönkkö and Timonen, 2019). The PTD and RTT dilution mimics atmospheric exhaust dilution conditions (Keskinen and Rönkkö, 2010), thus no additional treatment was required for fresh aerosol. The eDiluter, on the other hand, is closer to "primary aerosol" as the first ejector diluter is heated; however, when no sample treatment followed the eDiluter it is noted as "Fresh" in the results section whereas if it was followed by the thermodenuder it is denoted as "Primary", even though these should both be equivalent to primary. Finally, the aerosol sample was diluted to increase the flow rate and to match the BC concentration to atmospheric conditions.

The above-mentioned primary aerosol was created by removing semi-volatile compounds from particles using a thermodenuder (Amanatidis et al., 2018). A thermodenuder heats the aerosol (set to 265 °C in these measurements), then removes the vaporized gaseous compounds using an active carbon filter, leaving only solid particles to the aerosol sample. The thermodenuder causes some losses for the solid particles (Heikkilä et al., 2009), but they are not corrected for here, as all the instruments were measuring the same aerosol in parallel. In the generation of fresh aerosol, we had two different options, i.e., coating particles with hydrocarbon or sulfuric acid. These mimic situations where BC is released together with semi-volatile vapors which easily condense on particle surfaces during the cooling dilution of exhaust (Ristimäki et al., 2007; Rönkkö et al., 2013). The aged BC-containing aerosol was formed by adding benzene to the test aerosol and by conducting the sample through a PAM (Potential Aerosol Mass, Aerodyne Research Inc, US, (Kang et al., 2011) chamber. A small amount of CO was also added to the aerosol flow before PAM, in order to calculate an estimate for the extent of aging. The PAM chamber lights were operated at two different voltages, equivalent to 1 day and 5 days of aging, calculated using the change in CO concentration.

Table 1 gives an overview of the measurements conducted in this study. The first six rows relate to our first objective: instrument responses to black carbon with different sample treatments, whereas the final three rows are concerned with our second and third objectives: examining how the sample dilution affects results and whether the particles from a spark generator gives the same responses as soot from a

Table 1
Measurement matrix. This study included three sample treatments, three particle coating options, two dilution methods and two different settings for aerosol aging in secondary aerosol cases.

Particle source	Sample Treatment	Particle Coating	Dilution Type	Aerosol Age (Days)
Gas burner	Primary	None	PTD	–
Gas burner	Fresh	None	PTD	–
Gas burner	Fresh	Octacosane	PTD	–
Gas burner	Fresh	Sulfuric acid	PTD	–
Gas burner	Secondary	Benzene	PTD	1
Gas burner	Secondary	Benzene	PTD	5
Gas burner	Primary	None	eDiluter	–
Gas burner	Fresh[a]	None	eDiluter	–
Spark generator	Fresh	None	PTD	–
Spark generator	Fresh	Octacosane	PTD	–

[a] The eDiluter "fresh" should be identical to the primary, as it consists of a hot ejector diluter followed by room temperature dilution.

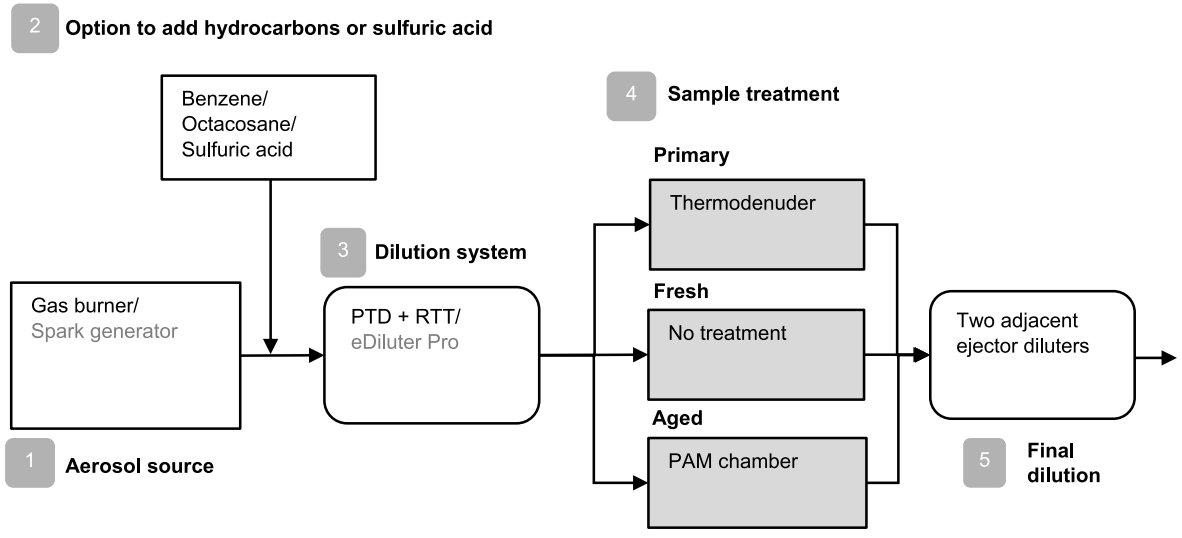

Fig. 1. A simple schematic of the aerosol production setup: 1. Aerosol source, 2. Option to add material for particle coating, 3. Initial dilution, 4. Sample treatment, 5. The final dilution stage, its function is to decrease particle concentration and to increase the aerosol volumetric flow rate. The final arrow leads to the instruments. A more detailed diagram of the aerosol production is included in the supplementary material, Fig. S1.

gas burner.

The first 31 measurements points had 60-min durations, as they included taking samples for the EC-OC analysis, as well as exposing cell cultures for a separate study (Hakkarainen et al., 2022). The later measurement points (32–48) were approximately 10 min each.

2.2. BC instrumentation

Table 2 provides a list of the BC instruments used in this study, along with the measurement method, time resolution and measurement range of each instrument. More detailed descriptions of the instruments are included below. We initially aimed to use the EC-OC analysis from the filter samples (first row in Table 2) as the reference value but, however, the collected particle masses were generally not enough for reliable results and, in the end, we only used one sample, which had the highest amount of collected mass (all the results are included in the supplementary data). In hindsight, the EC-OC collection should have been conducted from the un-diluted aerosol. The other option would have been to increase the measurement duration for each measurement point. Both options have their drawbacks: the first would leave some doubt whether the dilution changes the sample, and the second would increase the length of the study or reduce the measurement matrix.

2.2.1. Thermo-optical analysis of EC and OC

Elemental carbon (EC) and organic carbon (OC) were analyzed using a thermal-optical carbon analyzer (OCEC, Sunset Laboratory, Tigard, OR, USA, model 5 L, *EN 16909:2017, 2017*), in which temperature and gas atmosphere was adjusted while continuously monitoring a laser signal transmission through the sample matrix (Birch and Cary, 1996). In the first phase (He-phase), sample is heated in four steps up to 650 °C in inert helium atmosphere to remove OC. Some of the organics may be pyrolyzed (PC) during inert phase, and this is observed by a decrease of the laser signal. In the second phase (He/Ox-phase), oxygen (2%) is introduced together with helium, and the temperature is elevated in five steps up to 920 °C. Carbon is oxidized to CO_2, which is then converted to methane and detected by the Flame Ionization Detector (FID). The PC formed during the temperature program is compensated by determining the point (split) when the laser signal achieves its original value. Methane is used as an internal standard and a known quantity of it is injected at the end of each analysis. Sucrose was used as an external standard. The temperature protocol used was EUSAAR2 (Cavalli et al., 2010).

2.2.2. Aethalometer AE33

Two dual-spot aethalometer (AE33, Magee Scientific, Slovenia) were used to measure the aerosol light absorption seven different wavelengths (370–950 nm). The eBC was determined from data with a wavelength of 880 nm (Drinovec et al., 2015; Hansen et al., 1984), and all seven wavelengths were used together to calculate the absorption Ångström exponent (AAE). In the instruments, the flow rate was 5 L min^{-1} and the time resolution of the measurement was 1 s. The filter tape was PTFE-coated glass fiber filters (no. M8060). We utilized the default value of 1.39 for the multiple scattering enhancement factor *C*. It should be noted that there are also other recommendations for *C* in the literature (Yus-Díez et al., 2021). The default mass absorption coefficient (MAC) values were used. In AE33s, the simultaneous collection of particles on two spots in parallel at different flow rates allows dual-spot correction which is done internally by the instrument.

2.2.3. Micro-Aethalometer MA200

The 5-wavelength (880 nm, 625 nm, 528 nm, 470 nm, 375 nm) microAethalometer MA200 (microAeth® Model MA200, Aethlabs, San Francisco, CA, Liu et al. (2021)), measures eBC concentration using the aethalometer measurement technology. In the Micro-Aethalometer, the particles are collected onto PTFE filter tape with 17 sampling locations and automatic filter tape advance system allowing continuous measurements. Like the AE33, MA200 also uses two spots to allow for dual-spot correction. It has a flowrate of 150 mL per minute.

2.2.4. MAAP 5012

Multi-angle absorption photometers (MAAP, Thermo Electron Corporation, Model 5012, Petzold and Schönlinner, 2004) determine the absorption coefficient of particles deposited on a filter by a simultaneous measurement of transmitted and backscattered light. The value of the absorption coefficient is then converted to eBC mass concentration by the instrument firmware using a mass absorption cross section of 6.6 m^2 g^{-1} (Petzold and Schönlinner, 2004). In this study, the raw MAAP data was corrected according to the procedure described in Hyvärinen et al. (2013) to account for artifacts related to high concentration, and multiplied by 1.05 as it was noticed in 2005 that the real MAAP wavelength is 637 nm instead of the nominal 670 nm (Müller et al., 2011). The flow rate of the instruments in this study was 5 L min^{-1} and the time resolution of the measurement was 1 min.

2.2.5. SP-AMS

The Soot Particle Aerosol Mass Spectrometer (SP-AMS, Aerodyne, Onasch et al., 2012) is a real-time instrument (time resolution ~1 min, depending on the settings) capable of measuring the size resolved mass concentration of approximately 70 nm–700 nm particles and their chemical composition. In an AMS (Aerosol Mass Spectrometer) the aerosol is sampled through an aerodynamic lens to focus the beam of particles. The travel time of particles from the mechanical chopper to a vaporizer is recorded to enable mass size distribution measurement. The particles are then vaporized and ionized into ions with an electron gun. The ions are led through an electric field in a time-of-flight chamber, eventually hitting a detection plate where the charge carried by the particles is recorded, as well as the travel-time through the chamber, which gives the mass of the ion. The instrument output is the amount of signal at each mass per charge ratio (m/z), and each ratio corresponds to a different ion. The SP-AMS is otherwise the same instrument as the

Table 2
BC instruments used in this study.

	Manufacturer	Time resolution	Range ($\mu g/m^3$)	Method	Literature Reference
Lab OC-EC Aerosol Analyzer (model 5L, software ECOC1029, calculation Cal359)	Sunset Laboratories Inc.	Offline measurement	1–15 $\mu g/cm^2$	Thermo-optical analysis of sample collected on filter	EN 16909:2017 (2017) Range: https://www.sunlab.com/about-us/methodology/
Aethalometer (AE33)	Magee Scientific	1 s	0.01–100	Light transmission (880 nm)	Hansen et al. (1984)
Micro-Aeth (MA200)	AethLabs	1 s	0–1000	Light transmission (880 nm)	Liu et al. (2021)
MAAP (5012)	Thermo Scientific Inc.	1 min	0–180[a]	Light (637 nm) absorption and scattering	Müller et al. (2011); Petzold et al. (2005)
MSS	AVL	1 s	1-	Photoacoustic	Lack et al. (2006)
SP-AMS	Aerodyne Research Inc.	1 min	0.03-	Vaporization with laser, detection with ToF-MS	Onasch et al. (2012)

[a] Range given in the manual for 10-min time resolution; our study used 1 min resolution.

AMS, except it also includes a laser to vaporize refractory material like soot particles allowing them to be measured as rBC.

The SP-AMS raw data requires detailed data-handling. We used Igor 6.37, ToF-AMS Analysis Toolkit 1.62G and ToF-AMS HR analysis 1.22G. SP-AMSs were calibrated for the ionization efficiency (IE) with ammonium nitrate and relative ionization efficiency (RIE) of rBC with Regal black before the experiments. IEs were 8.77e-08 and 1.05e-07, and RIEs for rBC were 0.17 and 0.066 for the SP-AMS$_A$ and SP-AMS$_B$, respectively. Additionally, the size distribution calibration was performed with polystyrene latex beads. A collection efficiency of 1 was used throughout the experiments.

2.2.6. MSS 483

The Micro Soot Sensor (MSS, Model 483, AVL List GmbH) is an instrument designed to measure BC using the photoacoustic method (Patrick Arnott et al., 1999). It uses a laser at a wavelength of 808 nm to heat the particles. The MSS can measure a large range of concentrations, from 1 μg/m^3 to 50 mg/m^3. We ran the calibration check with an absorber window once per hour. The instrument needs to be manually turned back on after the calibration. Unfortunately, this was not always done in this study. Additionally, the MSS was not available for the full duration of the measurements, thus some of the data is missing.

2.3. Auxiliary measurements

In addition to the BC measurements, the aerosol was measured with several other instruments to determine the particle size distribution and concentration, as well as the concentration of gaseous compounds. Our main instrument for the particle size distribution was ELPI+ (Dekati Ltd.) which is an electrical low-pressure cascade impactor capable of measuring the aerodynamic size distribution of particles between 6 nm and 10 μm. We also used several CPCs (Condensation Particle Counters, Airmodus Ltd.) and SMPS systems (Scanning Mobility Particle Sizer, TSI Inc.); however, data from these instruments are used only to supplement the measurements with ELPI+. We measured the concentration of SO_2 with a gas analyzer (Environnement S.A.) to make sure that it was being oxidized by the DOC (Diesel Oxidation Catalyst). Similarly, the hydrocarbon concentration was measured with an FID (Flame Ionization Detector, Mocon Inc.) to verify that production remained relatively stable. Finally, aerosol light scattering and backscattering were measured using an integrated nephelometer (TSI, model 3563) at wavelengths 450, 550 and 700 nm (Anderson et al., 1996). The flow rate of the nephelometer was 5 L min^{-1} and the time resolution was 1 min. The truncation correction (Anderson and Ogren, 1998; Bond et al., 2009) was not made for the measured data since the particle sizes in the sample were <1.0 μm.

2.4. Calculation and Statistical methods

The raw data for each instrument was first processed to correct for differences in timestamps and conduct any instrument-specific corrections. We then gathered the data for each individual measurement and instrument, and calculated the mean, median and standard deviation. In the results section, the data points are median values, so as to ignore short interferences that may have been caused by activity in the laboratory. Because we did not have a reference value to compare results to, we calculated an overall mean result $\overline{BC}$ from the available data, using equation (1), to use as a value for comparison.

$$\overline{BC} = \overline{\overline{BC}_{aethalometers} + \overline{BC}_{MAAPs} + \overline{BC}_{MSS}} \quad (1)$$

Data from the SP-AMS instruments were not included in this overall mean, neither is MAAP data over 10 μg/m^3, as these results were clearly in disagreement with the rest of the data. The reasons for these discrepancies are discussed further in the next section.

Aethalometer data was used to calculate the AAE of each measurement sample. AAE gives an indication of how the coefficient for light absorption C_{abs} depends on the wavelength of light λ, as described by eq. (2). For BC the AAE is approximately one, but the exact value depends on particle size and varies with the source of the BC (Helin et al., 2021). The constant C_0 equals the absorption coefficient at a wavelength of 1 μm. We calculated the AAE value of our samples with eq. (3), using data from each of the seven aethalometer channels of different wavelengths.

$$C_{abs}(\lambda) = C_0 \lambda^{-AAE} \quad (2)$$

$$\Leftrightarrow \ln C_{abs}(\lambda) = \ln C_o - AAE \ln \lambda \quad (3)$$

In atmospheric studies, AAE is commonly used to estimate the amount of Brown Carbon in a sample. Here, we checked the sample treatment effect on the AAE (if any), and then investigated instrument performance dependency on the AAE.

3. Results & discussion

In this section, we first compare identical instruments to each other and then all instruments to the overall average result (calculated with eq. (1)). Results which were deemed uncertain from the comparison of the identical instruments were not included when calculating the overall mean values. Finally, we discuss the sources of uncertainty that could not be controlled by data processing.

3.1. Identical instruments compared

Fig. 2 shows the comparisons for pairs of identical instruments: Aethalometer, SP-AMS and MAAP. To separate the duplicate instruments, they were named A and B. We only had one MSS and one Micro-Aethalometer for the measurements, thus they are not included here.

Considering the comparison of identical instruments in Fig. 2, the aethalometers had the best result, with a slope close to one and a high correlation ($R^2 = 0.998$). There are some individual data points which stand out from the rest; these were measured with either fresh or aged test aerosol.

The correlation between the results measured with MAAPs was excellent up to 10 μg/m^3, but the results deviate at measurement points with larger concentrations. We also noted some problems during the measurements: after measuring a large concentration, the MAAPs would have a hysteresis effect, continuing to show high values for some time after the concentration was lowered again. When considering Fig. S5 results, which only include data points for the sample concentration less than 10 μg/m^3, the MAAPs had the best intercorrelation ($R^2 = 0.990$), and a slope of 1.03—very close to the one-to-one correlation curve.

The SP-AMS results are interesting, as it seems that the two instruments have different responses to the aged aerosol compared to the rest of the data points. Overall, SP-AMS$_B$ detected significantly less rBC than SP-AMS$_A$. The RIE values for rBC were very different for the two units, as SP-AMS$_A$ had a RIE more than a double of that of SP-AMS$_B$ leading to a higher BC sensitivity. Looking into the results further, we noticed that when the mass of organics relative to BC was high (mainly the aged aerosol cases), the SP-AMS$_B$ results for rBC increased relative to SP-AMS$_A$. The effect was prominent especially in the carbon fragment C_2^+, which can be from either from BC or organics. Typically, C_2^+ is counted as a fragment of BC in the SP-AMS mass spectra, however, in case of aged aerosol, it seemed to be mostly related to organics in SP-AMS$_B$ due to the poor sensitivity for rBC. By comparing the rBC size distributions from the two instruments, we were able to rule out the aerodynamic lens as having an impact on the discrepancies between the two instruments.

The EC results were separately analyzed by two labs, and the intercorrelation of the results was very good despite the low concentrations (equation of the fitted line $0.9407x + 0.0126$, $R^2 = 0.9533$).

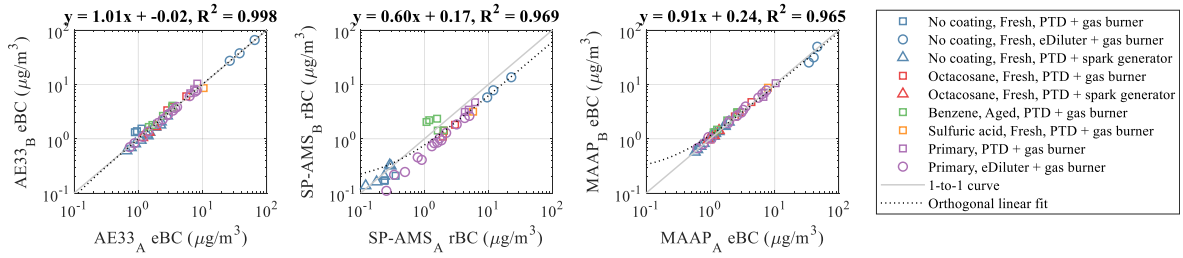

Fig. 2. Identical instruments (AE33, SP-AMS, MAAP) compared to each other. The black dotted line is the orthogonal linear regression fit for the data, and the equation for it is shown on top of each subfigure, along with the correlation coefficient (R^2). The light grey line shows the one-to-one curve.

3.2. Comparison of all instruments to an overall mean

In this section, each instrument is compared separately to the overall mean result, $\overline{BC}$, calculated using eq. (1). Fig. 3 includes all measurements which were successful for all eight instruments. The related particle size distributions are shown in Fig. S2 and the BC data is also presented numerically in Table S1. As mentioned previously, the thermo-optical EC analysis from filters was unsuccessful due to small collection amounts (<1 μg/cm^2), as shown in Fig. S3 where the EC analysis results are plotted against eBC measured with an aethalometer. Overall, the EC concentrations are smaller than eBC concentrations, but there is a clear trend of converging with the aethalometer results with increasing concentration. The highest collected mass, corresponding to test points 04_primary and 05_primary, was the only one compared to other results, shown in Fig. S4. The thermo-optical analysis gave a slightly lower result for EC content than the eBC methods and a higher value than the SP-AMS results; however, no conclusions can be drawn from this very limited data.

The overall median concentration was roughly 3 μg/m^3, and the total measurement range was roughly from 0.8 to 60 μg/m^3. This range covers ambient air applications, and the median value is quite close to the average exposure level. From Fig. 3, it is easy to see that the SP-AMS instruments showed clearly lower (about 50%) values compared to the other instruments. All the other methods gave nearly the same median result (rounding to one significant digit). The SP-AMS is based on a different measurement technique from others: it measures BC on a mass basis whereas all the other instruments determine BC either optically or photo-acoustically. It has been shown in previous studies that the SP-AMS results compare well with other mass-based instruments like Single Particle Soot Photometer (Tasoglou et al., 2018), or even with the MAAP if the SP-AMS is calibrated for BC by using the MAAP (Onasch et al., 2012).

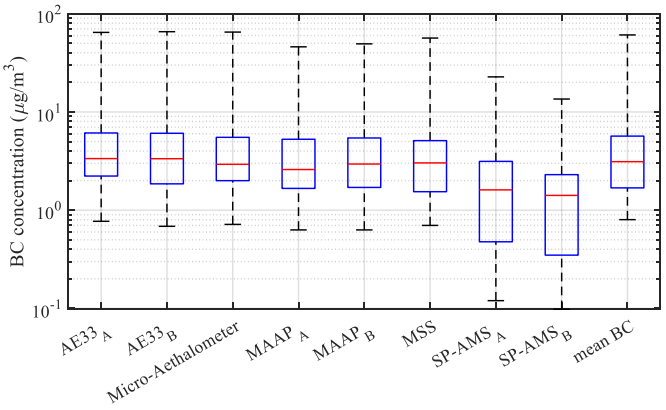

Fig. 3. Boxplot of all the results which were successful for all instruments (N = 27) and the mean, calculated according to equation (1). The median (red line), 25th and 75th percentiles (blue box) and minimum and maximum values (whiskers) of BC concentrations for each instrument are shown.

Fig. 4 aims to show whether the sample treatment, particle coating or particle source are associated with any differences between instruments. Fig. 4 contains all measured data points, and the results from each instrument are plotted against the overall mean. The aethalometers, MAAPs and MSS had good agreement for most of the measurement situations. Overall, the aethalometers reported the largest values, possibly due to their inability to differentiate between scattering and absorption. The MSS response to the spark generator samples was smaller than the aethalometer and MAAP responses, but many of these were situations of small concentrations, below the reported detection limit of MSS of 1 μg/m^3. The aerodynamic diameter of the spark-generated particles was also smaller than the gas burner particles (Fig. S2), which perhaps influenced the MSS response as in the study by Kinsey et al. (2019).

The SP-AMS instruments reported less than half the concentration of the other instruments. One reason is the that the transmission of particles through the aerodynamic lens is dependent on particle size, at 70 nm roughly half of particles are transmitted and the transmission improves with increasing size up to 100 nm, then decreases again past 350 nm (Liu et al., 2007). However, aside from the spark-generated particles, the count median particle size was larger than 70 nm (Fig. S2, Table S1), meaning much more than half of the mass should have been able to enter the instruments. Another reason for the smaller BC concentrations from the SP-AMS is the collection efficiency applied. We used a CE of 1 while in a study by Willis et al. (2014) a CE of less than unity was measured for BC particles, the CE depending on the thickness of organic coating.

Fig. S7 shows the relative error for the results measured with each instrument at primary measurement points with PTD + RTT dilution and double ejector dilution (eDiluter). Three points between 5 and 10 μg/m^3 were chosen for each dilution type, and the average relative error of these three points was calculated. There were no systematic major differences between dilution type in the relative errors. The range of AAE values from the two dilution methods were also similar, 0.9–1.13 for the eDiluter and 0.84–1.10 for the PTD + RTT (Fig. S6, Table S1).

As the dilution method did not affect results, the next figures include data from both PTD + RTT dilution and the double-ejector dilution methods. The spark generator as a particle source on the other hand created aerodynamically small particles, with larger AAEs (Fig. S6). There was a bit more variation between instrument responses, especially the MSS and SP-AMS. It is however unclear whether the variation in the instrument responses was due to the smaller concentrations, the smaller aerodynamic size, or the particle source. In any case, Fig. 5 only includes measurements with the gas burner as the aerosol source.

Fig. 5 shows the dependency of the relative error (relative difference of a particular instrument's result compared to the mean) on the primary particle count median diameter (CMD), the measured AAE and the ratio of sulfates and organics to BC. See Fig. S8, Fig. S9 and Fig. S10 for dependency on the mean BC concentration, particle number concentration and measurement duration, respectively. The corresponding primary particle CMD was chosen for the plot instead of the fresh/aged distribution CMD, as those had also nucleation mode particles and the CMD was then significantly affected by particles not containing BC.

Based on Fig. 5, the particle size had at most a very slight effect on

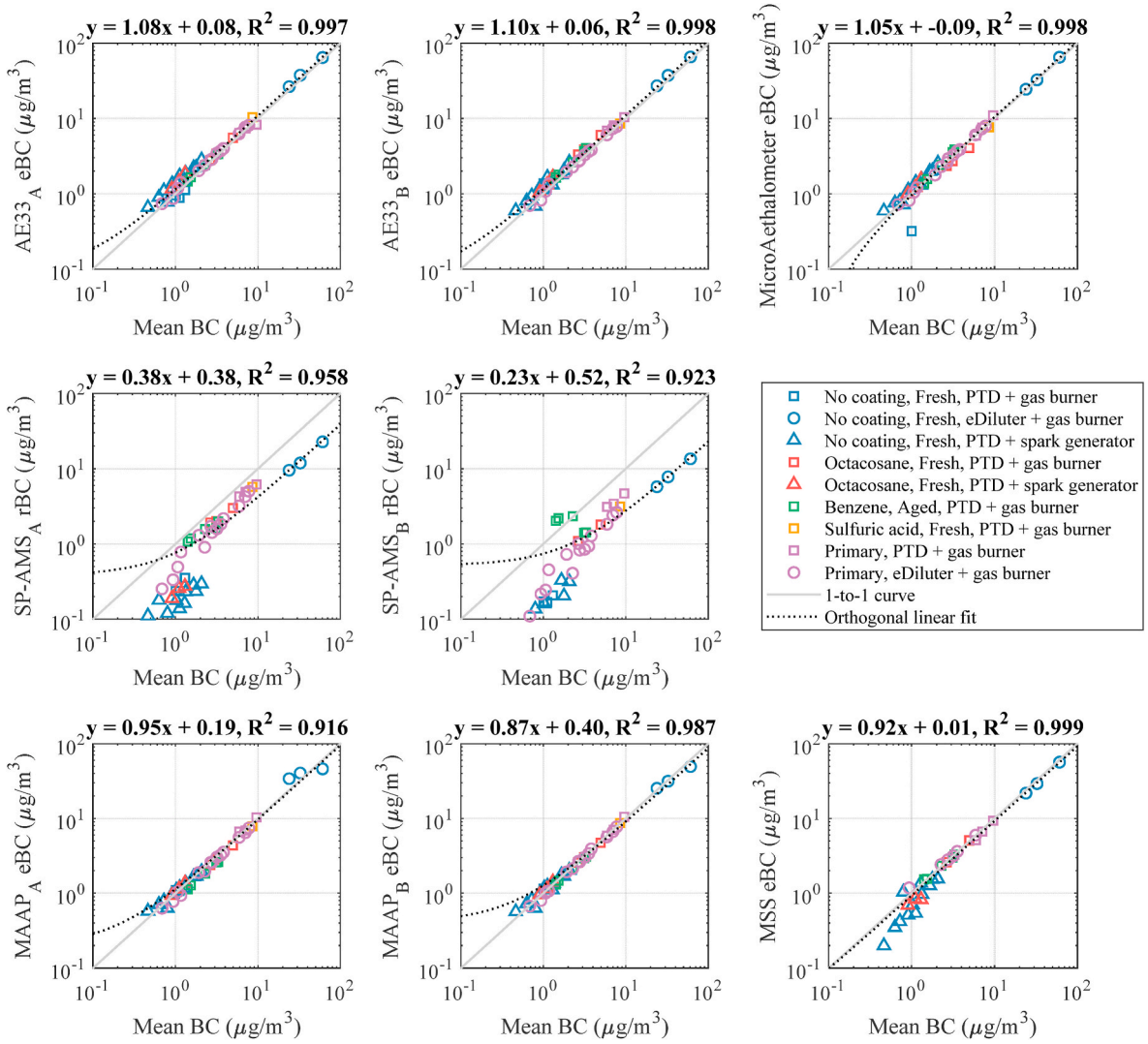

Fig. 4. The correlations between each BC result and the overall mean, $\overline{BC}$.

the results; results indicated a change in relative error only when measuring rBC with SP-AMS$_A$ so that the increase of particle size resulted to decrease of deviation of the result from instrument mean. This observation was perhaps linked with the increased ratio of organics and sulfate compared to BC leading to better BC detection efficiency when using SP-AMSs. However, the thicker organic coating of the BC particles also increases the collection efficiency of particles due to narrowed beam width (Willis et al., 2014). This trend was seen with both SP-AMS instruments, but it was clearer with SP-AMS$_B$. The SP-AMS dependency on AAE might be due to the relationship between AAE and particle size (inverse relationship, see Fig. S11).

We would have expected to see eBC values increase compared to rBC with thicker coatings due to the lensing effect; however, this was most likely obscured by the increased efficiency of the SP-AMS.

3.3. Uncertainties to consider

Here we have estimated the accuracy components related to BC measurement methods to generate a robust assessment of the possible measurement uncertainty.

There is no standardized reference method for BC measurement that is applicable both in measurements of ambient BC and BC emissions. However, standardized OC/EC method (EN 16909:2017) is widely used in ambient aerosol studies and the uncertainties of that method have been studied and reported comprehensively (Brown et al., 2017). In this study, we collected the generated particles for the OC/EC analyses using this method; however, we did not manage to collect enough particulate mass on filter for accurate results, the minimum being 1 μg/cm^2. In general, this (too low collected particulate mass) can be seen as a typical source of uncertainty in OC/EC measurements in emission studies where the collection time is typically limited, and the temporal variation of the concentrations is significantly bigger than in ambient measurements. For instance, the utilization of standardized OC/EC method to get reliable data for each driving mode of standardized engine emission test cycle is practically impossible due to the short available time windows (few minutes) and dilution needed for engine exhaust. No standardized BC emission measurement techniques will be suitable for all BC emission sources. However, e.g., MSS has been chosen as a standard reference instrument for certification of aircraft engines (SAE E−31 AIR 6241, ARP6320) (Aakko-Saksa et al., 2022).

There are several quite general uncertainty sources in BC measurements, some of them applicable for all BC instruments and some for certain techniques. First, the uncertainties of all the measurement techniques are dependent on accuracy of mass or volume flow measurements of sample. In general, the sample flow of the instrument should be calibrated traceably to ensure the comparability of results. Secondly, measurement conditions (pressure, temperature, RH etc.) can affect either the functioning of the instrument (e.g., sample flow can

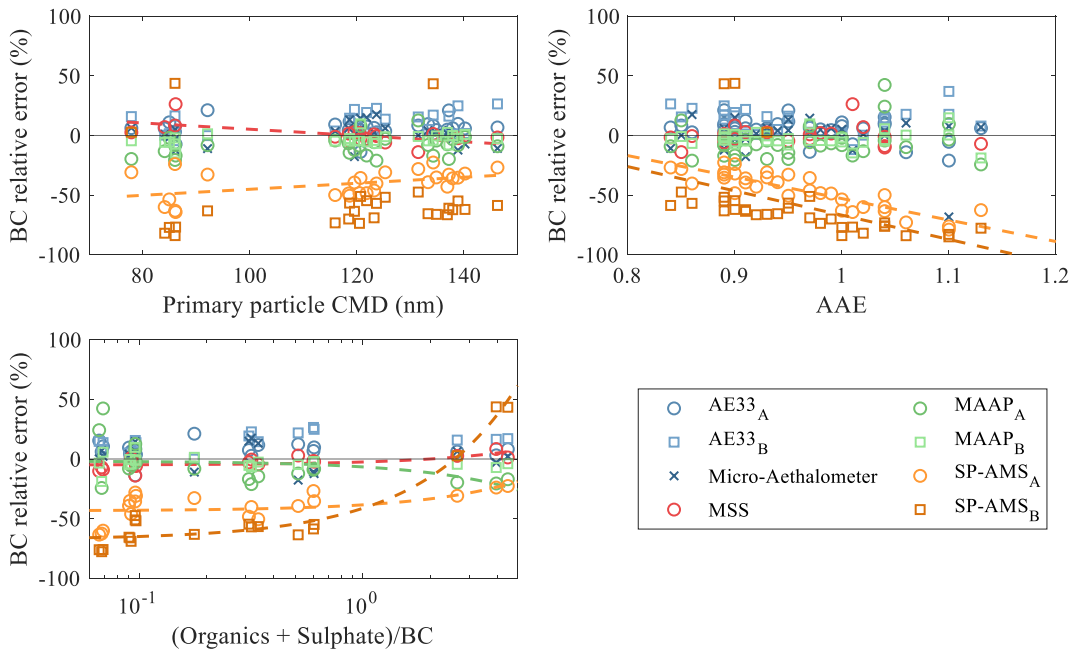

Fig. 5. The relative error in BC plotted against the CMD of the primary particle distribution, measured AAE and organics + sulfate ratio to BC. Only the measurements with the gas burner are included in these plots. The comparison to organics and sulfate relative to BC was limited to measurement points with at least 0.5 μg/m3 of sulfate + organics. Best fit lines are shown where a correlation of $R^2 = 0.15$ or better was found.

differ from calibrated values when sampling from low pressure or from high temperature exhaust) or the representativeness of result itself (e.g., cooling of aerosol sample can cause the change the BC particle size due to the condensing compounds and affect the detection of BC). One example of this is the need for the aethalometer to adjust to new conditions (Cuesta-Mosquera et al., 2021). Thirdly, the studied aerosols can contain compounds that interfere with the BC measurement. The interfering compounds can affect differently for different measurement methods, e.g., the semivolatile compounds of vehicle exhaust may not affect significantly the BC measured by MSS directly from tailpipe, but they can significantly alter the absorption characteristics of diluted exhaust and thus the eBC results measured at roadside optically by aethalometers and MAAP. In general, combustion processes generate lot of compounds with different absorption and volatility characteristics which can affect the interpretation of BC measurement results (e.g., so called brown carbon substances absorb at lower wavelengths (Li et al., 2019) and affect the total absorption of the aerosol but they are not considered to BC). Furthermore, uncertainty in the parameters used in data analyses and used corrections (e.g., absorption coefficients) can affect the uncertainty of final BC measurement results (see e.g., Asmi et al., 2021; Yus-Díez et al., 2021).

4. Summary of results

This study had an overall positive outcome: observed differences between the results measured with different instruments were relatively small for the laboratory generated aerosol using the gas burner. The main discrepancies were due to already known limitations presented in literature. However, aerosol characteristics (particle size, chemistry, concentration range, etc.) from different sources and in different places can differ significantly from the test aerosol used in this study, and thus further instrument comparison studies are still needed. Additionally, the compared instruments (all except the SP-AMS and thermo-optical filter analysis) use similar detection methods.

Results from the eDiluter and PTD were similar, the choice of dilution did not affect results. This is of course a positive result, as it means the dilution method does not significantly alter the characteristics of the produced BC.

Regardless of the variation of the test aerosol treatment in this study (primary soot vs fresh aerosol vs aged aerosol), the MSS, MAAPs and aethalometers all showed very similar results. The spark generator cases were the only clear discrepancy, with MSS reporting somewhat smaller concentrations. This could be due to the small aerodynamic size of the particles, the small concentrations or some other property related to the spark generator. The spark generator produced small particles with a larger AAE than particles from the gas burner. It is not clear from these measurements whether the smaller size caused the large AAE or some unknown property. The MAAPs had some difficulty when measuring very high concentrations, and during the measurement campaign we had to wait some time for the MAAPs to recover before moving to the next measurement point. While high concentrations (~20 μg/m^3 and above) are rare in ambient air, care should be taken to ensure sufficient dilution in emission measurements.

The SP-AMS instruments both reported significantly smaller concentrations than the other instruments. Partially, this is explained by particle losses in the aerodynamic lens, though the losses alone cannot account for the full discrepancy. Additionally, the parameters used in data analysis, such as collection efficiency, may affect the concentrations. It should also be noted here that the SP-AMS instrument is based on a very different measurement technique from the other as it measures rBC on mass-based whereas others are optical or photo-acoustic methods. The two SP-AMS instruments were also different in comparison to each other, this was found to be due to the differences in the laser vaporizing efficiency. This emphasizes that the SP-AMS is an advanced research grade instrument which needs accurate calibrations and laser alignment. Based on our study, the absolute amount of rBC can be difficult to infer from the SP-AMS results; however, the SP-AMS was the only instrument in the study that can measure the size distribution of rBC as well as the chemical composition of the particle coating.

Information on the comparability of different commonly used BC measurement methods is of utmost importance for air quality modeling and BC emission inventories, as well as when deciding about upcoming legislation e.g., BC emission limits for shipping. Furthermore, more data and knowledge on BC is urgently needed to reduce the uncertainties related to aerosol effects on climate change. In general, the results of our study can decrease these uncertainties in climate studies not only by

providing tools for more accurate and comparable BC measurements in the future but also when the existing BC data is interpreted.

Author contributions

Laura Salo: Investigation, Data Curation, Visualization, Writing – Original Draft; Karri Saarnio: Conceptualization, Writing - Review & Editing; Sanna Saarikoski: Investigation, Data Curation, Writing - Review & Editing, Funding acquisition; Kimmo Teinilä: Investigation, Data Curation, Writing - Review & Editing; Luis Barreira: Investigation, Writing - Review & Editing; Petteri Marjanen: Investigation, Writing - Review & Editing; Sampsa Martikainen: Investigation, Writing - Review & Editing; Helmi Keskinen: Data Curation, Writing - Review & Editing; Katja Mustonen: Data Curation, Writing - Review & Editing; Teemu Lepistö: Investigation, Writing - Review & Editing; Päivi Aakko-Saksa: Conceptualization, Writing - Review & Editing, Supervision, Henri Hakkarainen: Investigation, Writing - Review & Editing; Tobias Pfeiffer: Investigation, Resources, Writing - Review & Editing; Pasi Jalava: Investigation, Writing - Review & Editing; Panu Karjalainen: Investigation, Writing - Review & Editing; Jorma Keskinen: Conceptualization, Supervision, Writing - Review & Editing; Niina Kuittinen: Writing - Review & Editing, Project Administration; Hilkka Timonen: Conceptualization, Writing - Review & Editing, Supervision, Funding acquisition; Topi Rönkkö: Conceptualization, Writing - Review & Editing, Supervision, Funding acquisition.

Declaration of competing interest

The authors declare that they have no known competing financial interests or personal relationships that could have appeared to influence the work reported in this paper.

Acknowledgements

Financial support from Black Carbon Footprint project funded by Business Finland (Grant 528/31/2019) and participating companies and municipal actors and by European Union Horizon 2020 research and innovation program under grant agreement No 814978 (TUBE). Support from Academy of Finland Flagship funding (grant no. 337552, 337551) and the project Black and Brown Carbon in the Atmosphere and the Cryosphere (BBrCAC) (grant nr. 341271) is gratefully acknowledged.

We would also like to thank Dekati for lending an eDiluter and an ELPI + for these measurements, Airmodus for providing an AND Nanoparticle Diluter, AVL for providing and sharing expertise regarding the MSS and VSParticle for lending the VSP G1 spark generator.

We want to thank Dr. Wilbert Vrijburg from VSParticle for offering his expertise in the measurements with the spark generator.

Appendix A. Supplementary data

Supplementary data to this article can be found online at https://doi.org/10.1016/j.apr.2024.102088.

References

Aakko-Saksa, P., Kuittinen, N., Murtonen, T., Koponen, P., Aurela, M., Järvinen, A., Teinilä, K., Saarikoski, S., Barreira, L.M.F., Salo, L., Karjalainen, P., Ortega, I.K., Delhaye, D., Lehtoranta, K., Vesala, H., Jalava, P., Rönkkö, T., Timonen, H., 2022. Suitability of different methods for measuring black carbon emissions from marine engines. Atmosphere 13. https://doi.org/10.3390/atmos13010031.

Amanatidis, S., Ntziachristos, L., Karjalainen, P., Saukko, E., Simonen, P., Kuittinen, N., Aakko-Saksa, P., Timonen, H., Rönkkö, T., Keskinen, J., 2018. Comparative performance of a thermal denuder and a catalytic stripper in sampling laboratory and marine exhaust aerosols. Aerosol Sci. Technol. 6826, 1–13. https://doi.org/10.1080/02786826.2017.1422236.

Anderson, T.L., Covert, D.S., Marshall, S.F., Laucks, M.L., Charlson, R.J., Waggoner, A.P., Ogren, J.A., Caldow, R., Holm, R.L., Quant, F.R., Sem, G.J., Wiedensohler, A., Ahlquist, N.A., Bates, T.S., 1996. Performance characteristics of a high-sensitivity, three-wavelength, total Scatter/backscatter nephelometer. J. Atmos. Ocean. Technol. 13, 967–986. https://doi.org/10.1175/1520-0426(1996)013<0967:PCOAHS>2.0.CO;2.

Anderson, T.L., Ogren, J.A., 1998. Determining aerosol radiative properties using the TSI 3563 integrating nephelometer. Aerosol Sci. Technol. 29, 57–69. https://doi.org/10.1080/02786829808965551.

Asmi, E., Backman, J., Servomaa, H., Virkkula, A., Gini, M.I., Eleftheriadis, K., Müller, T., Ohata, S., Kondo, Y., Hyvärinen, A., 2021. Absorption instruments inter-comparison campaign at the Arctic Pallas station. Atmos. Meas. Tech. 14, 5397–5413. https://doi.org/10.5194/amt-14-5397-2021.

Birch, M.E., Cary, R.A., 1996. Elemental carbon-based method for monitoring occupational exposures to particulate diesel exhaust. Aerosol Sci. Technol. 25, 221–241. https://doi.org/10.1080/02786829608965393.

Bond, T.C., Covert, D.S., Müller, T., 2009. Truncation and angular-scattering corrections for absorbing aerosol in the TSI 3563 nephelometer. Aerosol Sci. Technol. 43, 866–871. https://doi.org/10.1080/02786820902998373.

Bond, T.C., Doherty, S.J., Fahey, D.W., Forster, P.M., Berntsen, T., Deangelo, B.J., Flanner, M.G., Ghan, S., Kärcher, B., Koch, D., Kinne, S., Kondo, Y., Quinn, P.K., Sarofim, M.C., Schultz, M.G., Schulz, M., Venkataraman, C., Zhang, H., Zhang, S., Bellouin, N., Guttikunda, S.K., Hopke, P.K., Jacobson, M.Z., Kaiser, J.W., Klimont, Z., Lohmann, U., Schwarz, J.P., Shindell, D., Storelvmo, T., Warren, S.G., Zender, C.S., 2013. Bounding the role of black carbon in the climate system: a scientific assessment. J. Geophys. Res. Atmospheres 118, 5380–5552. https://doi.org/10.1002/JGRD.50171.

Briggs, N.L., Long, C.M., 2016. Critical review of black carbon and elemental carbon source apportionment in Europe and the United States. Atmos. Environ. 144, 409–427. https://doi.org/10.1016/j.atmosenv.2016.09.002.

Brown, R.J.C., Beccaceci, S., Butterfield, D.M., Quincey, P.G., Harris, P.M., Maggos, T., Panteliadis, P., John, A., Jedynska, A., Kuhlbusch, T.A.J., Putaud, J.-P., Karanasiou, A., 2017. Standardisation of a European measurement method for organic carbon and elemental carbon in ambient air: results of the field trial campaign and the determination of a measurement uncertainty and working range. Environ. Sci. Processes Impacts 19, 1249–1259. https://doi.org/10.1039/C7EM00261K.

Cavalli, F., Viana, M., Yttri, K.E., Genberg, J., Putaud, J.-P., 2010. Toward a standardised thermal-optical protocol for measuring atmospheric organic and elemental carbon: the EUSAAR protocol. Atmos. Meas. Tech. 3, 79–89. https://doi.org/10.5194/amt-3-79-2010.

Cuesta-Mosquera, A., Močnik, G., Drinovec, L., Müller, T., Pfeifer, S., Minguillón, M.C., Briel, B., Buckley, P., Dudoitis, V., Fernández-García, J., Fernández-Amado, M., Ferreira De Brito, J., Riffault, V., Flentje, H., Heffernan, E., Kalivitis, N., Kalogridis, A.-C., Keernik, H., Marmureanu, L., Luoma, K., Marinoni, A., Pikridas, M., Schauer, G., Serfozo, N., Servomaa, H., Titos, G., Yus-Díez, J., Zioła, N., Wiedensohler, A., 2021. Intercomparison and characterization of 23 Aethalometers under laboratory and ambient air conditions: procedures and unit-to-unit variabilities. Atmos. Meas. Tech. 14, 3195–3216. https://doi.org/10.5194/amt-14-3195-2021.

Drinovec, L., Jagodič, U., Pirker, L., Škarabot, M., Kurtjak, M., Vidović, K., Ferrero, L., Visser, B., Röhrbein, J., Weingartner, E., Kalbermatter, D.M., Vasilatou, K., Bühlmann, T., Pascale, C., Müller, T., Wiedensohler, A., Močnik, G., 2022. A dual-wavelength photothermal aerosol absorption monitor: design, calibration and performance. Atmos. Meas. Tech. 15, 3805–3825. https://doi.org/10.5194/amt-15-3805-2022.

Drinovec, L., Močnik, G., Zotter, P., Prévôt, A.S.H., Ruckstuhl, C., Coz, E., Rupakheti, M., Sciare, J., Müller, T., Wiedensohler, A., Hansen, A.D.A., 2015. The "dual-spot" Aethalometer: an improved measurement of aerosol black carbon with real-time loading compensation. Atmos. Meas. Tech. 8, 1965–1979. https://doi.org/10.5194/amt-8-1965-2015.

EN 16909:2017, 2017. Ambient Air - Measurement of Elemental Carbon (EC) and Organic Carbon (OC) Collected on Filters.

Hakkarainen, H., Salo, L., Mikkonen, S., Saarikoski, S., Aurela, M., Teinilä, K., Ihalainen, M., Martikainen, S., Marjanen, P., Lepistö, T., Kuittinen, N., Saarnio, K., 2022. Black carbon toxicity dependence on particle coating : measurements with a novel cell exposure method. Sci. Total Environ. 838 https://doi.org/10.1016/j.scitotenv.2022.156543.

Hansen, A.D.A., Rosen, H., Novakov, T., 1984. The aethalometer — an instrument for the real-time measurement of optical absorption by aerosol particles. Sci. Total Environ. 36, 191–196. https://doi.org/10.1016/0048-9697(84)90265-1.

Heikkilä, J., Rönkkö, T., Lähde, T., Lemmetty, M., Arffman, A., Virtanen, A., Keskinen, J., Pirjola, L., Rothe, D., 2009. Effect of open channel filter on particle emissions of modern diesel engine. J. Air Waste Manag. Assoc. 59, 1148–1154. https://doi.org/10.3155/1047-3289.59.10.1148.

Helin, A., Virkkula, A., Backman, J., Pirjola, L., Sippula, O., Aakko-Saksa, P., Väätäinen, S., Mylläri, F., Järvinen, A., Bloss, M., Aurela, M., Jakobi, G., Karjalainen, P., Zimmermann, R., Jokiniemi, J., Saarikoski, S., Tissari, J., Rönkkö, T., Niemi, J.V., Timonen, H., 2021. Variation of absorption Ångström exponent in aerosols from different emission sources. J. Geophys. Res. Atmospheres 126, e2020JD034094. https://doi.org/10.1029/2020JD034094.

Hyvärinen, A.-P., Vakkari, V., Laakso, L., Hooda, R.K., Sharma, V.P., Panwar, T.S., Beukes, J.P., van Zyl, P.G., Josipovic, M., Garland, R.M., Andreae, M.O., Pöschl, U., Petzold, A., 2013. Correction for a measurement artifact of the Multi-Angle Absorption Photometer (MAAP) at high black carbon mass concentration levels. Atmos. Meas. Tech. 6, 81–90. https://doi.org/10.5194/amt-6-81-2013.

Kalbermatter, D.M., Močnik, G., Drinovec, L., Visser, B., Röhrbein, J., Oscity, M., Weingartner, E., Hyvärinen, A.-P., Vasilatou, K., 2022. Comparing black-carbon- and aerosol-absorption-measuring instruments – a new system using lab-generated soot

coated with controlled amounts of secondary organic matter. Atmos. Meas. Tech. 15, 561–572. https://doi.org/10.5194/amt-15-561-2022.
Kanaya, Y., Komazaki, Y., Pochanart, P., Liu, Y., Akimoto, H., Gao, J., Wang, T., Wang, Z., 2008. Mass concentrations of black carbon measured by four instruments in the middle of Central East China in June 2006. Atmos. Chem. Phys. 8, 7637–7649. https://doi.org/10.5194/acp-8-7637-2008.
Kang, E., Toohey, D.W., Brune, W.H., 2011. Dependence of SOA oxidation on organic aerosol mass concentration and OH exposure: experimental PAM chamber studies. Atmos. Chem. Phys. 11, 1837–1852. https://doi.org/10.5194/acp-11-1837-2011.
Keskinen, J., Rönkkö, T., 2010. Can real-world diesel exhaust particle size distribution be reproduced in the laboratory? A critical review. J. Air Waste Manag. Assoc. 60, 1245–1255. https://doi.org/10.3155/1047-3289.60.10.1245.
Kinsey, J.S., Corporan, E., Pavlovic, J., DeWitt, M., Klingshirn, C., Logan, R., 2019. Comparison of measurement methods for the characterization of the black carbon emissions from a T63 turboshaft engine burning conventional and Fischer-Tropsch fuels. J. Air Waste Manag. Assoc. 69, 576–591. https://doi.org/10.1080/10962247.2018.1556188, 1995.
Klimont, Z., Kupiainen, K., Heyes, C., Purohit, P., Cofala, J., Rafaj, P., Borken-Kleefeld, J., Schöpp, W., 2017. Global anthropogenic emissions of particulate matter including black carbon. Atmos. Chem. Phys. 17, 8681–8723. https://doi.org/10.5194/acp-17-8681-2017.
Lack, D.A., Lovejoy, E.R., Baynard, T., Pettersson, A., Ravishankara, A.R., 2006. Aerosol absorption measurement using photoacoustic spectroscopy: sensitivity, calibration, and uncertainty developments. Aerosol Sci. Technol. 40, 697–708. https://doi.org/10.1080/02786820600803917.
Li, H., Lamb, K.D., Schwarz, J.P., Selimovic, V., Yokelson, R.J., McMeeking, G.R., May, A. A., 2019. Inter-comparison of black carbon measurement methods for simulated open biomass burning emissions. Atmos. Environ. 206, 156–169. https://doi.org/10.1016/j.atmosenv.2019.03.010.
Lighty, J.S., Veranth, J.M., Sarofim, A.F., 2000. Combustion aerosols: factors governing their size and composition and implications to human health. J. Air Waste Manag. Assoc. 50, 1565–1618. https://doi.org/10.1080/10473289.2000.10464197.
Liu, P.S.K., Deng, R., Smith, K.A., Williams, L.R., Jayne, J.T., Canagaratna, M.R., Moore, K., Onasch, T.B., Worsnop, D.R., Deshler, T., 2007. Transmission efficiency of an aerodynamic focusing lens system: comparison of model calculations and laboratory measurements for the aerodyne aerosol mass spectrometer. Aerosol Sci. Technol. 41, 721–733. https://doi.org/10.1080/02786820701422278.
Liu, X., Hadiatullah, H., Zhang, X., Hill, L.D., White, A.H.A., Schnelle-Kreis, J., Bendl, J., Jakobi, G., Schloter-Hai, B., Zimmermann, R., 2021. Analysis of mobile monitoring data from the microAeth (R) MA200 for measuring changes in black carbon on the roadside in Augsburg. Atmos. Meas. Tech. 14, 5139–5151. https://doi.org/10.5194/amt-14-5139-2021.
Liu, Y., Yan, C., Zheng, M., 2018. Source apportionment of black carbon during winter in Beijing. Sci. Total Environ. 618, 531–541. https://doi.org/10.1016/j.scitotenv.2017.11.053.
Michelsen, H.A., Colket, M.B., Bengtsson, P.-E., D'Anna, A., Desgroux, P., Haynes, B.S., Miller, J.H., Nathan, G.J., Pitsch, H., Wang, H., 2020. A review of terminology used to describe soot formation and evolution under combustion and pyrolytic conditions. ACS Nano 14, 12470–12490. https://doi.org/10.1021/acsnano.0c06226.
Müller, T., Henzing, J.S., de Leeuw, G., Wiedensohler, A., Alastuey, A., Angelov, H., Bizjak, M., Collaud Coen, M., Engström, J.E., Gruening, C., Hillamo, R., Hoffer, A., Imre, K., Ivanow, P., Jennings, G., Sun, J.Y., Kalivitis, N., Karlsson, H., Komppula, M., Laj, P., Li, S.-M., Lunder, C., Marinoni, A., Martins dos Santos, S., Moerman, M., Nowak, A., Ogren, J.A., Petzold, A., Pichon, J.M., Rodriquez, S., Sharma, S., Sheridan, P.J., Teinilä, K., Tuch, T., Viana, M., Virkkula, A., Weingartner, E., Wilhelm, R., Wang, Y.Q., 2011. Characterization and intercomparison of aerosol absorption photometers: result of two intercomparison workshops. Atmos. Meas. Tech. 4, 245–268. https://doi.org/10.5194/amt-4-245-2011.
Onasch, T.B., Trimborn, A., Fortner, E.C., Jayne, J.T., Kok, G.L., Williams, L.R., Davidovits, P., Worsnop, D.R., 2012. Soot particle aerosol mass spectrometer: development, validation, and initial application. Aerosol. Sci. Technol. 46, 804–817. https://doi.org/10.1080/02786826.2012.663948.
Pant, P., Habib, G., Marshall, J.D., Peltier, R.E., 2017. PM2.5 exposure in highly polluted cities: a case study from New Delhi, India. Environ. Res. 156, 167–174. https://doi.org/10.1016/j.envres.2017.03.024.
Patrick Arnott, W., Moosmüller, H., Fred Rogers, C., Jin, T., Bruch, R., 1999. Photoacoustic spectrometer for measuring light absorption by aerosol: instrument description. Atmos. Environ. 33, 2845–2852. https://doi.org/10.1016/S1352-2310(98)00361-6.
Petzold, A., Kramer, H., Schönlinner, M., 2002. Continuous measurement of atmospheric black carbon using a multi-angle absorption photometer. Environ. Sci. Pollut. Res. Special Is 78–82.
Petzold, A., Niessner, R., 1996. Photoacoustic soot sensor for in-situ black carbon monitoring. Appl. Phys. B 63, 191–197. https://doi.org/10.1007/BF01095272.
Petzold, A., Ogren, J.A., Fiebig, M., Laj, P., Li, S.-M., Baltensperger, U., Holzer-Popp, T., Kinne, S., Pappalardo, G., Sugimoto, N., Wehrli, C., Wiedensohler, A., Zhang, X.-Y., 2013. Recommendations for reporting "black carbon" measurements. Atmos. Chem. Phys. 13, 8365–8379. https://doi.org/10.5194/acp-13-8365-2013.
Petzold, A., Schloesser, H., Sheridan, P.J., Arnott, W.P., Ogren, J.A., Virkkula, A., 2005. Evaluation of multiangle absorption photometry for measuring aerosol light absorption. Aerosol Sci. Technol. 39, 40–51. https://doi.org/10.1080/027868290901945.
Petzold, A., Schönlinner, M., 2004. Multi-angle absorption photometry—a new method for the measurement of aerosol light absorption and atmospheric black carbon. J. Aerosol Sci. 35, 421–441. https://doi.org/10.1016/j.jaerosci.2003.09.005.
Räisänen, P., Merikanto, J., Makkonen, R., Savolahti, M., Kirkevåg, A., Sand, M., Seland, Ø., Partanen, A.-I., 2022. Mapping the dependence of black carbon radiative forcing on emission region and season. Atmos. Chem. Phys. 22, 11579–11602. https://doi.org/10.5194/acp-22-11579-2022.
Ristimäki, J., Vaaraslahti, K., Lappi, M., Keskinen, J., 2007. Hydrocarbon condensation in heavy-duty diesel exhaust. Environ. Sci. Technol. 41, 6397–6402. https://doi.org/10.1021/es0624319.
Rönkkö, T., Lähde, T., Heikkilä, J., Pirjola, L., Bauschke, U., Arnold, F., Schlager, H., Rothe, D., Yli-Ojanperä, J., Keskinen, J., 2013. Effects of gaseous Sulphuric acid on diesel exhaust Nanoparticle formation and characteristics. Environ. Sci. Technol. 47, 11882–11889. https://doi.org/10.1021/es402354y.
Rönkkö, T., Saarikoski, S., Kuittinen, N., Karjalainen, P., Keskinen, H., Järvinen, A., Mylläri, F., Aakko-Saksa, P., Timonen, H., 2023. Review of black carbon emission factors from different anthropogenic sources. Environ. Res. Lett. 18, 033004 https://doi.org/10.1088/1748-9326/acbb1b.
Rönkkö, T., Timonen, H., 2019. Overview of sources and characteristics of nanoparticles in urban traffic-influenced areas. J. Alzheimers Dis. JAD 72, 15–28. https://doi.org/10.3233/JAD-190170.
Saarikoski, S., Niemi, J.V., Aurela, M., Pirjola, L., Kousa, A., Rönkkö, T., Timonen, H., 2021. Sources of black carbon at residential and traffic environments obtained by two source apportionment methods. Atmos. Chem. Phys. 21, 14851–14869. https://doi.org/10.5194/acp-21-14851-2021.
Sedlacek, A.J., 2017. Single-Particle Soot Photometer (SP2) Instrument Handbook.
Slowik, J.G., Cross, E.S., Han, J.-H.H., Davidovits, P., Onasch, T.B., Jayne, J.T., Williams, L.R., Canagaratna, M.R., Worsnop, D.R., Chakrabarty, R.K., Moosmüller, H., Arnott, W.P., Schwarz, J.P., Gao, R.S., Fahey, D.W., Kok, G.L., Petzold, A., 2007. An inter-comparison of instruments measuring black carbon content of soot particles. Aerosol Sci. Technol. 41, 295–314. https://doi.org/10.1080/02786820701197078.
Snelling, D.R., Smallwood, G.J., Liu, F., Gülder, Ö.L., Bachalo, W.D., 2005. A calibration-independent laser-induced incandescence technique for soot measurement by detecting absolute light intensity. Appl. Opt. 44, 6773–6785. https://doi.org/10.1364/AO.44.006773.
Stone, R., 2002. Air pollution. Counting the cost of London's killer smog. Science 298, 2106–2107. https://doi.org/10.1126/science.298.5601.2106b.
Tasoglou, A., Subramanian, R., Pandis, S.N., 2018. An inter-comparison of black-carbon-related instruments in a laboratory study of biomass burning aerosol. Aerosol Sci. Technol. 52, 1320–1331. https://doi.org/10.1080/02786826.2018.1515473.
ten Brink, H.M., Hitzenberger, R., Virkkula, A., 2022. On the historic exposure levels of Elemental Carbon from vehicle diesel exhaust based on "diesel smoke" concentrations. Atmos. Environ. 286, 119177 https://doi.org/10.1016/j.atmosenv.2022.119177.
Vander Wal, R.L., Weiland, K.J., 1994. Laser-induced incandescence: development and characterization towards a measurement of soot-volume fraction. Appl. Phys. B 59, 445–452. https://doi.org/10.1007/BF01081067.
Wang, R., Tao, S., Balkanski, Y., Ciais, P., Boucher, O., Liu, J., Piao, S., Shen, H., Vuolo, M.R., Valari, M., Chen, H., Chen, Y., Cozic, A., Huang, Y., Li, B., Li, W., Shen, G., Wang, B., Zhang, Y., 2014. Exposure to ambient black carbon derived from a unique inventory and high-resolution model. Proc. Natl. Acad. Sci. 111, 2459–2463. https://doi.org/10.1073/pnas.1318763111.
Willis, M.D., Lee, A.K.Y., Onasch, T.B., Fortner, E.C., Williams, L.R., Lambe, A.T., Worsnop, D.R., Abbatt, J.P.D., 2014. Collection efficiency of the soot-particle aerosol mass spectrometer (SP-AMS) for internally mixed particulate black carbon. Atmos. Meas. Tech. 7, 4507–4516. https://doi.org/10.5194/amt-7-4507-2014.
World Health Organization, 2021. WHO Global Air Quality Guidelines: Particulate Matter (PM2.5 and PM10), Ozone, Nitrogen Dioxide, Sulfur Dioxide and Carbon Monoxide. World Health Organization.
Yus-Díez, J., Bernardoni, V., Močnik, G., Alastuey, A., Ciniglia, D., Ivančič, M., Querol, X., Perez, N., Reche, C., Rigler, M., Vecchi, R., Valentini, S., Pandolfi, M., 2021. Determination of the multiple-scattering correction factor and its cross-sensitivity to scattering and wavelength dependence for different AE33 Aethalometer filter tapes: a multi-instrumental approach. Atmos. Meas. Tech. 14, 6335–6355. https://doi.org/10.5194/amt-14-6335-2021.